Geotechnical Challenges for the Numerical Prediction of the Settlement Behaviour of Foundations in Rosenheim's Seeton

Roberto Cudmani, Daniel Rebstock, and Joshua Schorr(✉)

Zentrum Geotechnik, Technical University of Munich, Munich, Germany
joshua.schorr@tum.de

Abstract. The Rosenheimer Basin in the alpine region near the German-Austrian border is a deep ancient glacial lake, which has been filled with fine-grained sediments over the course of the past 10.000 to 100.000 years. Due to the rapid economic growth in the region over the last few decades, the high population density and the increasing utilisation of infrastructure in the region a significant demand for development exists, particularly for structures with large loads. The design and construction of such structures represents a significant challenge for engineers due to the sensitive soft, fine-grained lacustrine sediments. This article focusses on the conception and design of a cable-stayed bridge pylon in Rosenheim. The foundation consists of bored piles connected to a pile cap, with additional displacement piles and vertical drains for soil improvement. As the stiffness and strength of the sensitive lacustrine sediments are strongly reduced due to the disturbances caused by pile installation, displacement piles in combination with vertical drains around the piles are prescribed in order to re-consolidate the soil ("soil healing") and increase the shaft friction after the pile installation. In order to take into account the effect of the soil disturbance and the healing effect of the soil improvements on the foundation behaviour realistically, high quality pile loading tests were carried out. Based on the results of laboratory and field tests, and the simulation of the single pile loading tests using a visco-hypoplasticity constitutive model, a 3D Finite-Element Model was developed and calibrated to predict the time-dependent behaviour of the mixed foundation. The numerical prediction shows that the serviceability requirements of the foundation can be fulfilled and the scheduled underpinning of the superstructure to compensate the foundation settlements will likely not be required prior to 50 years of operation. An extensive monitoring program will be implemented during the construction to validate and, if necessary, to adjust the numerical model to realistically predict the long-term deformation behaviour of the bridge foundations.

1 Introduction

As part of the new western by-pass road B15, Westtangente Rosenheim, two bridges line have been planned with a total length of around 670 m to cross the Mangfall River and the Mangfall canal, the industrial area Aicherpark and a railway. The bridges consist of a cable-stayed bridge with a maximum span between the pylons of 100 m, and a 480 m long, multi-span beam bridge with spans varying between 20 m and 31 m (Figs. 1 and 2).

T. Triantafyllidis (Ed.): *Recent Developments of Soil Mechanics and Geotechnics in Theory and Practice*, LNACM 91, pp. 323–346, 2020.
https://doi.org/10.1007/978-3-030-28516-6_17

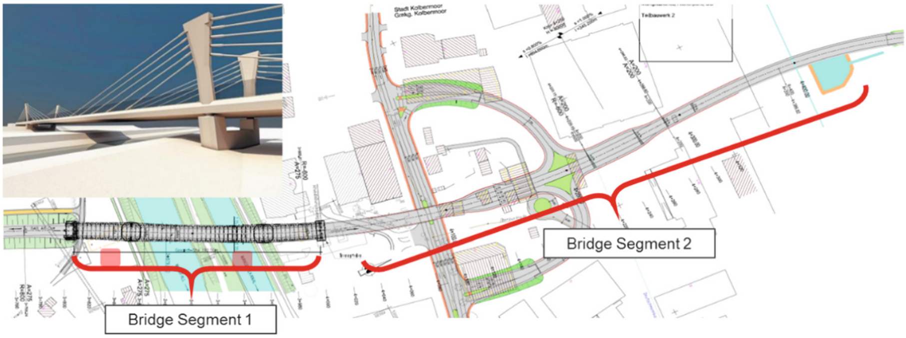

Fig. 1. Bridge structures crossing over the Mangfall river, Mangfall canal, the Aicherpark industrial estate and the Holzkirchen - Rosenheim railway line: Bridge Segment 1 (Mangfall bridge): Ingenieurbüro Grassl GmbH (Structural design) | Reinhart + Partner Architekten und Stadtplaner (Visualisation); Bridge Segment 2 (Aicherpark bridge): SSF Ingenieure AG (Structural design).

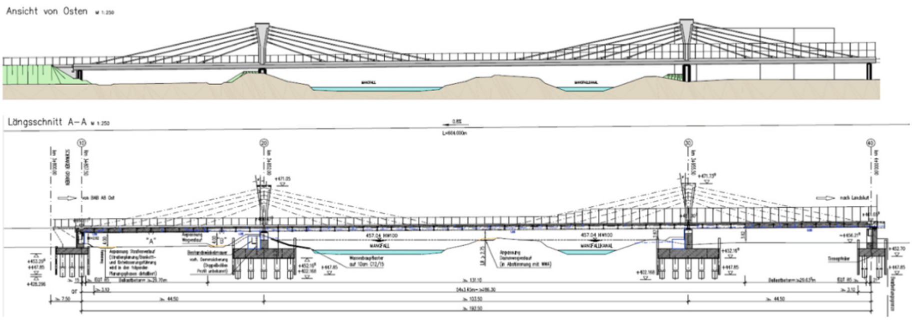

Fig. 2. Bridge Segment 1: Cable-stayed bridge over the Mangfall river and Mangfall canals (side view); Ingenieurbüro Grassl GmbH (Structural design) | Reinhart + Partner Architekten und Stadtplaner (Visualisation).

A particular challenge for the realisation of the project is the subsoil, which consists of quaternary, sensitive, very soft, low plastic and fine-grained lacustrine deposits, the so-called "Seeton" of the Rosenheim sedimentary basin. Due to the thickness of the lacustrine clayey sandy silt layer, down to depths of approx. 150 m in the vicinity of the bridge construction site, floating foundations are required to transfer the bridge loads to the subsoil. Due to the viscous behaviour and low bearing capacity, fulfilment of the geotechnical limit and serviceability states for this soil is a difficult task, especially for the foundation of the pylon. The relatively high loads necessitate the use of bored piles, despite the fact that the installation of the piles cause a considerable disturbance to the subsoil, considerably affecting their bearing behaviour and reducing their bearing capacity.

The development of an innovative floating foundation to account for the complex subsoil conditions in Rosenheim, with focus on the three dimensional Finite Element Analysis (FEA) of the foundation behaviour is presented in this article. Firstly, the main conclusions of the comprehensive soil investigations that were carried out to assess the mechanical time-dependent behaviour of the clay are described. Subsequently, the additional requirements for the piling and concreting works, which were specified to reduce the disturbance of the sensitive soil as well as the results of three high-quality static pile loading tests are described. These results are used to calibrate the numerical model of the foundation and to validate the application of the FEA to simulate its bearing behaviour. Using the pylon foundation as example, the strategy for the fulfilment of the geotechnical design requirements for the limit and the serviceability state of the floating foundation will be discussed. The observation method will be applied in order to deal with uncertainties related to the settlement prediction over the lifespan of the described bridges in the lacustrine sediments.

With this aim, in addition to the FEA of the foundation behaviour, a comprehensive monitoring program will be implemented, during both the construction and operation of the bridge. The observation method allows for the employment of remediation works, such as the possibility to lift the bridge superstructure, if the admissible settlements of the foundation, as per the structural design are exceeded. With the help of the FEA model, the time-dependent foundation settlement can be assessed and the appropriate time for lifting of the bridge can be scheduled.

2 Geological and Geotechnical Subsoil Conditions

The area around Rosenheim lies in the catchment area of the Inn River. In the last ice age about 100.000 to 1.000.000 years ago, the Ur-Inn was a huge glacial valley. It consisted of a solid ice layer at the base of the Alps surrounded by moraine, which was pushed by the glacier. After the Ice Age, the moraine dammed the meltwater of the glacier to form the Rosenheimer Lake (surface area of around 420 km^2), which over time, was continuously filled with fluviatile sediments transported by the Inn. Depending on the grain size and the flow velocity the fine-grained soils consisting of silt, clays and fine sands with thicknesses of up to 300 m were deposited in the ancient lake. About 12,000 years ago, the moraine barrier north of the village "Wasserburg am Inn" was broken through resulting in a complete loss of the water contained in the lake. Overlying the lacustrine clay or "Seeton" is a cover layer of alluvial sediments consisting of gravel, sand, and silt mixtures of varying thicknesses is typically encountered.

At the location of the construction site, the Seeton, with a thickness of 150 m, is covered by such a cover layer with a thickness of 6 m to 8 m and consisting of silty gravel. According to geotechnical investigations, the lacustrine sediments at the site consist mainly of silt and clayey silt interbedded with very fine sand layers, which can seldom be identified by a visual inspection. According to the results of the soil classification tests, the Seeton can be classified predominantly as a low plastic clayey-silt with a very soft to soft consistency (liquid limit $w_L = 0{,}38$, plastic limit $w_P = 0{,}20$, natural water content $w_n = 0{,}30$ to 0,38). Typically, the Seeton has a very small permeability in the vertical direction ($k_v \leq 10^{-8}$ m/s) due to the presence of the fine-grained layers, while the permeability in the horizontal direction, which is controlled by the permeability of the interbedded sand layers, is up to two orders of magnitude larger.

The investigation of the subsoil in the vicinity of the pylons, especially in the area of the pile loading tests, consisted of a total of 3 boreholes, 15 CPT and pressiometer tests using the cone-pressiometer testing device (CPTM), with final depths of up to

70 m. Furthermore, 31 CPT tests were carried out up to a depth of 70 m in locations corresponding to the piers of the multi-span bridge. Additionally, soil samples were retrieved with a tube sampler for the determination of the index properties and the investigation of the soil mechanical behaviour of the Seeton in the laboratory.

The shear strength c_u derived from the cone penetration resistance q_c by means of the common empirical relationship described in Fig. 3 shows a linear increase with depth which is typical for normal consolidated clays. These c_u values were confirmed by the results of the undrained triaxial compression tests carried out on the "disturbed" samples retrieved from the boreholes. The relationship $\Delta c_u / \Delta \sigma'_0 = 0.1$ (σ'_0: in situ vertical effective stress) corresponds to the lower boundary of the range of the data encountered in the literature for soft clays (e.g. Hansbo 1957), which typically increase from about 0.1 to 0.4 for a limit liquid of w_L = 0.25 to 0.8. These interbedded thin sand layers are most probably the cause for the sudden increases in the cone resistance, as repeatedly observed in Fig. 3.

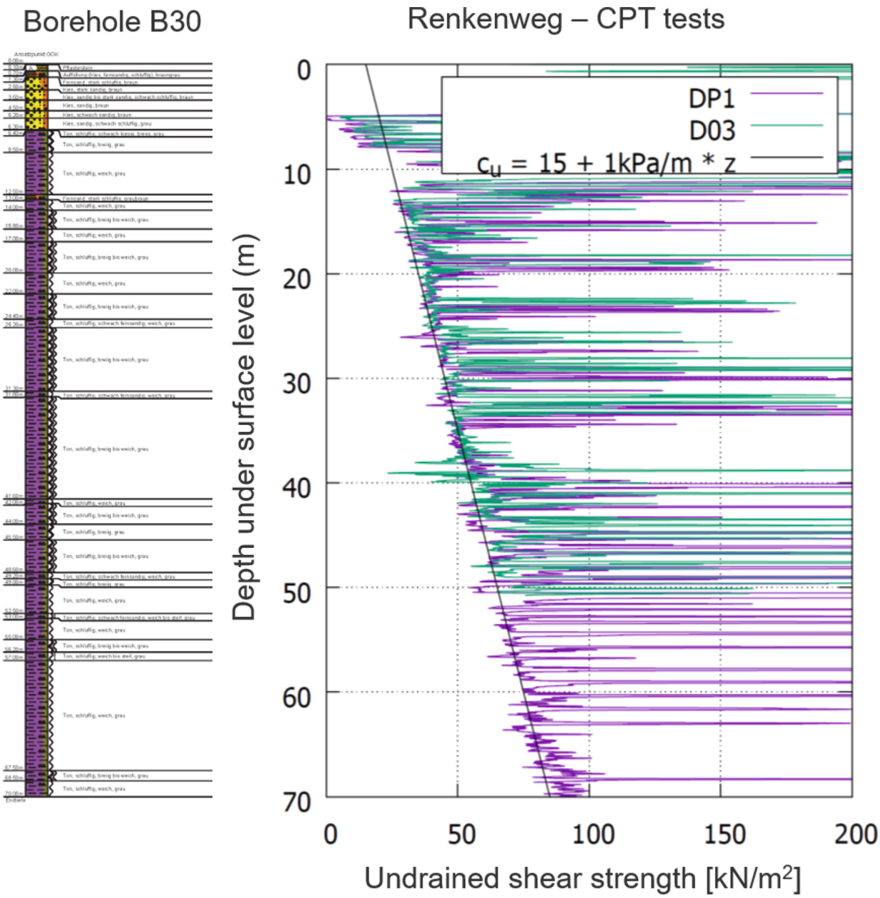

Fig. 3. Example of the determination of the undrained shear strength from the cone penetration resistance $c_u = (q_c - \sigma_{v0})/N_k$ with $N_k = 15$.

The mechanical behaviour of the Seeton is rate dependent. The viscosity index (Leinenkugel 1976) determined in the laboratory according to Krieg (2000) was found to be $I_v = 0.03$. Therefore, the time-dependent soil behaviour and the loading rate must be considered for a realistic assessment of the deformations of the bridge foundations.

3 First and Second Pile Loading Test Campaign

In the original geotechnical report of the project, in which the authors of the article were not involved, a floating pile foundation was recommended to transfer the loads of the pylon and the piers to the ground. For the foundation design, a characteristic value of the skin friction of $q_s = 30$ kN/m^2 and a negligible end bearing $q_b = 0$ was recommended. Furthermore, it was assumed that an increase of skin friction of $q_s = 60$ kN/m^2 could be realizable by post-grouting of the pile shaft. It was stated that the skin friction q_s applied in the design must be confirmed by pile loading tests (PLT).

With this aim, two pile loading campaigns were carried out between October 2015 and September 2016 - without the participation of the authors. In the first campaign, three bored piles were subjected to tension loads and in the second campaign, eight bored piles were installed in two test fields and subjected to compression loads. The test piles had a diameter of 1.2 m and lengths of between 17.5 m and 27.5 m (1st campaign) and 30.5 m (2nd campaign). Due to the thickness and the planned location of the pile caps below the ground surface, the most part of the cover layer will be excavated and hence, the bearing behaviour of the piles will be determined predominantly by the shaft and end bearing resistance in the Seeton. For this reason, measures to eliminate or at least to reduce the skin friction in the upper gravel layer during the pile testing had to be carried out. The measures used to achieve this consisted of welding a thin steel tube to the reinforcement in the area of the upper gravel layer in order to create a gap between this tube and the temporary casing used to drill the borehole. It was intended, that after withdrawal of the temporary casing, the gravel would close the annular gap and become looser, leading to a reduction of the friction angle and the horizontal stresses, resulting in a reduction in the skin friction.

In both, the first and second PLT campaigns, the skin friction in the Seeton layer assumed for the design could not be confirmed. The evaluation also showed that the highest skin friction was mobilised in the cover layer, where the skin friction should have been eliminated. The reason for the ineffectiveness of the measures to eliminate skin friction became apparent once the pile heads were uncovered: the annular gap between the steel tube and the gravel layer had been filled with concrete. Instead of a reduction, this led to an increase of the skin friction in the cover layer.

With the aim of improving the bearing capacity, in four of the eight tested piles, additional measures were tested consisting of (post) grouting and (post) installation of vertical drains around the piles. A systematic improvement of the pile bearing capacity with respect to the piles without any treatment was not observed. The measured bearing capacity, defined as the pile resistance for a displacement equivalent to 10% of the pile diameter, varied between 2,000 kN and 4,800 kN. After subtracting the skin friction in the cover layer and the end bearing, the skin friction in the Seeton varied between 0 and 25 kN/m^2, with a mean value below $q_s = 10$ kN/m^2. Despite the relative homogenous soil conditions encountered at the site, the large variations of the measured pile skin friction meant that it was not possible to extrapolate the PLT data to the design of the bridge foundations. Therefore, the pile loading test results did not fulfill an essential condition for the experimental determination of the pile bearing capacity, according to the applicable standards and recommended guidelines published by the geotechnical community. Even assuming reproducibility of the PLT results, adopting a characteristic skin friction $q_s = 10$ kN/m^2 for the foundation design would have led to pile lengths of more than 100 m making construction of the bridge extremely difficult from a technical, and most certainly infeasible from an economical point of view.

Ultimately, it was concluded that neither the evaluation of the skin friction and the load bearing behaviour of the tested piles nor the extrapolation of the skin friction to the foundation piles were reliable based on the results of the two PLT campaigns. For this reason, the execution of a third PLT campaign was recommended to finally assess the technical and economic feasibility of a floating pile foundation of the bridge.

4 Third Pile Testing Campaign

4.1 Concept Und Pile Instrumentation

The third PPB campaign was conceived by the authors in cooperation with the technical department of BAUER Spezialtiefbau GmbH and involved three test piles (P09, P10 and P11) and six reaction piles (R19 to R24) with a nominal diameter of D = 1.2 m. The length of the test piles were 30 m (P09 and P10) and 60 m (P11). Four reaction piles with D = 1.2 m and a length of 40 m were used to load the piles. The new test field was located adjacent to the previous test field at Aicherpark, such that the three existing reaction piles (R10, R13 and R16) from the second PPB campaign could be reused (Fig. 4).

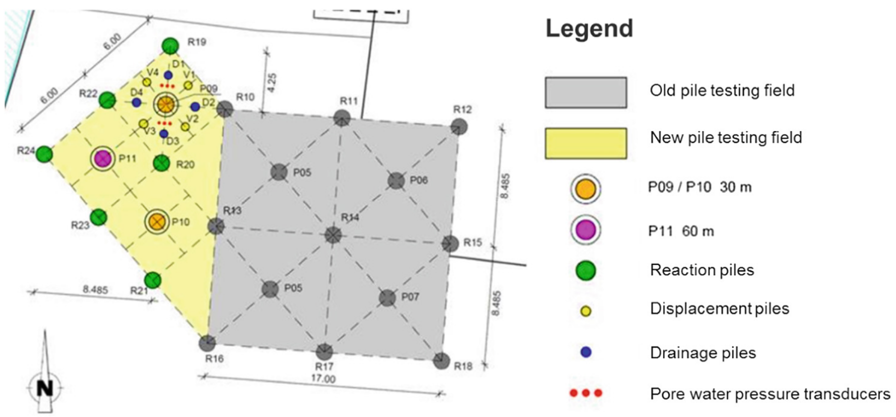

Fig. 4. Third static pile testing campaign – Test field and pile layout, including the reaction piles.

In order to evaluate the mobilized pile resistance over the depth, the piles were instrumented with concrete strain gauges (BVG) and extensometers (EXT). These two independent systems provided a redundancy in the determination of the normal forces, affording a certain level of quality control over the strain measurements. Three Geokon "Sister Bars" were installed at each of the BVG cross-sections. Each pile has two BVG cross-sections in the upper gravel layer, where the skin friction has been eliminated, for calibration purposes. The extensometer used was the retrievable "Model 1300" from Geokon (Fig. 5). The extensometers are pneumatically anchored in steel pipes that were installed in the piles. A vibrating wire displacement transducer is mounted below each anchor point. The piles P09 and P10 were each equipped with two extensometer strings with four and five anchoring points, respectively. For pile P11, the two short extensometer strands were converted into a long strand with eight anchor points.

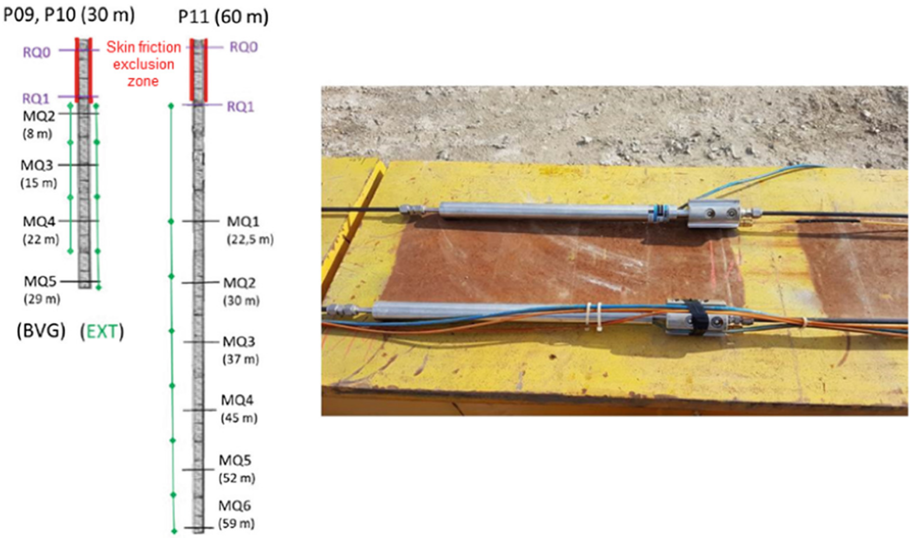

Fig. 5. Instrumentation of the test piles – left: locations of the instrumented cross sections with strain gages (BVG); and right: retrievable extensometer (EXT) with pneumatically expandable anchors and vibrating wire strain gauges.

4.2 Technical Specification for Pile Installation

The three test piles and the six new reaction piles were installed between Jan. 10th and Feb. 7th 2017. The drilling rig used was a BG 46 with an additional casing oscillator (Fig. 6, left). In order to reduce the disturbance to the sensitive Seeton as much as possible, different technical requirements were specified for the piling works. These included; drilling under water load to prevent hydraulic failure, pre-advancing the casing to a depth $\geq 2 \cdot D_s \approx 2.4$ m below the bottom of the bore-head (also when the planned final depth is reached) as well as the limitation of the drilling and withdrawal speed of the drilling bucket. In order to stabilise the base of the borehole after reaching the final depth, an additional 0.5 m thick gravel layer was deposited at the base of the piles and compacted with the drill bucket prior to the installation of the reinforcement.

Fig. 6. BAUER BG46 with: casing oscillator and water inflow (left) and ring auger to eliminate the skin friction in the cover layer (right).

The pile installation process was subjected to careful documentation. During concreting, the installed or removed casing and tremie pipe lengths, the actual concrete volume, the current concrete level and the height of the reinforcement cage were all continuously monitored. The reinforcement cage for the test piles settled about 65 cm for P09 and P10, and 90 cm for P11. The major part of these deformations occurred just after withdrawal of the first liner segment to above the bottom of the borehole, after pouring the first concrete load. The settlement resulted from the gap left by the casing below the bottom of the borehole and the consolidation of the Seeton under the weight of the reinforcement cage.

The exclusion of the skin friction in the area of the gravelly surface layer was carried out with a new and innovative system. It consisted of drilling a borehole with a diameter of 2.0 to a depth of about 7 m below the ground level, with an approx. embedment of 0.5 m into the Seeton and filling the borehole with plastic concrete. Next, a special ring auger (Fig. 6, right) was used to drill a hole of greater than 1.2 m in diameter. This meant that following the normal installation of the pile, an annular gap between the pile and the plastic concrete is created, ensuring the complete elimination of the skin friction in the cover layer as the remaining plastic concrete ring supports the surrounding soil and the annular gap is filled with water.

4.3 "Healing" the Seeton After Pile Installation

Following the installation of test pile P09 (see site plan in Fig. 4) four full displacement piles V1 to V4 (CMC: Controlled Modulus Columns, System Menard GmbH), with a diameter of 0.4 m and a length of 28 m below ground level, were installed with the aim of compensating for the disturbance of the Seeton due to the pile installation. The displacement auger which was used, is shown in Fig. 7.

Fig. 7. Displacement auger used to install the CMC piles.

In the plan view, the CMCs were installed symmetrically around the pile, within a relative short distance from the pile shaft, in order to induce a re-consolidation of the Seeton and thereby increase the skin friction. In addition, four vertical drains D1 to D4 were installed prior to the installation of the CMCs with the aim of accelerating consolidation. The consolidation process was monitored by pore pressure transducers installed in and around the pile.

4.4 Loading System and Instrumentation of the Pile Head

A reaction system consisting of two steel beams with a span of 8.5 m was used to apply the test loads. As mentioned before, the reaction loads were transferred to the four reaction piles by two GEWI bars per reaction pile (Fig. 8). The reaction system was designed for a capacity of 11 MN. The load was applied by means of a hydraulic jack, which allowed a variable oil intake and a SDA 1100 hydraulic cylinder (max. load of 11,000 kN at a nominal pressure of 692 bar). The load was kept constant by means of an electronic contact pressure gauge (accuracy of ±0.5 bar). The force was recorded by an electronic load cell. The vertical pile head deformations were recorded using three digital displacement transducers. Two additional electric displacement transducers were used to check the horizontal displacement of the pile head. In addition, the tensile forces in the GEWI bars were recorded by means of electronic load cells in order to check that the load was evenly distributed. The entire test data were recorded and stored digitally and could be evaluated and displayed in real time. To check the functionality and the results of the main measuring system; the settlements of the pile heads, the measurement bridges, the reaction piles and a fixed point (outside the area of influence of the pile loading apparatus) were recorded manually using a Leica DNA03 digital dumpy level.

Fig. 8. Pile loading test (pile P10 is depicted) – load transfer beams and loading setup, vehicle containing the measurement equipment and a surveyor's dumpy level.

4.5 Execution of the Pile Loading Tests

The pile loading tests took place between March and May, 2017 and consisted of two phases for all three piles. In the first, load-controlled phase (CLT: constant load test), the piles were loaded in increments of approx. 250 kN, at the start of the test and approx. 100 kN, towards the end of the test. During these loading stages, the creep coefficients were determined with the following relationship:

$$k_s = \frac{(S_2 - S_1)}{\log t_2 - \log t_1}$$

Where s is the Settlement of pile head and t is the time since begin of the load stage. The coefficients were determined in intervals of 20 min. According to the recommendations of the German geotechnical society, EA-Piles (2012), the load was only increased when the creep coefficient became constant or began to decrease with time and the velocity of the pile head displacement was lower than 0.005 mm/min. Aside from the determination of the load-settlement behaviour of the pile, the aim of the load-controlled test phase was to investigate the time-dependent developments of the settlements under constant load and the possibility of a creep failure at high loading levels. Unstable behaviour, indicated by an increase in the settlement velocity and the creep coefficient with time, was not observed up to the maximum load of the load-controlled phase (load leading to a pile head settlement of 0.1 D). To the contrary, despite the fact that quite large creep coefficients of up to 20 mm were recorded near the maximum CLT increments, for long observation times, the creep coefficient remained either constant or decreased with time (Fig. 9). The load-controlled test phase was carried out until the limit displacement of 0.1•D ≈ 12 cm according to EA-Piles (2012), was reached. An overview of the load-controlled test phases for the three test piles can be seen in Table 1.

Table 1. Overview of the load controlled phases

		P09 (L = 30 m, with soil improvement)	P10 (L = 30 m, without soil improvement)	P11 (L = 60 m, without soil improvement)
Max. Test force controlled phases	[kN]	3257	1990	6509
Number of loading steps	[–]	20	12	26
Total testing time	[h]	~328	~205,5	~274,5
	[d]	~13,5	~8,5	~11,5

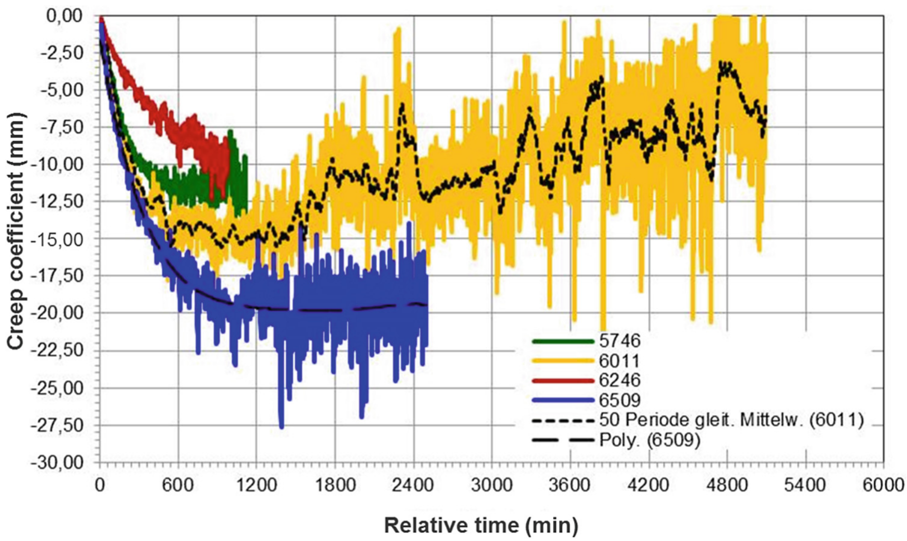

Fig. 9. Pile test P11 – Variation of the creep coefficient during loading stage time for the last four loading stages.

The load-controlled test phase was followed by a second, velocity-controlled phase (CRT: constant rate test) that included three "velocity jump tests". The initial velocity at the pile head of approx. 0.6 mm/min was increased by the factors 3.5, 0.5 and 7 in the jump tests. The velocity-controlled test phase was finished once the maximum displacement range of the hydraulic cylinder of 25 cm was reached. From the jump tests, the pseudo-viscosity index could be determined Krieg and Goldscheider (1998):

$$I_v = \frac{\ln(R_1(u)/R_2(u))}{\ln(\dot{u}_1/\dot{u}_2)} = 0.027 - 0.032$$

Where $R_i(u)$ is the pile resistance that would develop for the velocity $\dot{u}_i$ of the pile head settlement at a vertical displacement u_i. In Fig. 10, the results of the CRT and the CLT phases are presented for the pile P09. The results show that the load-settlement response from the CRT phase can be used to derive the load-settlement response for the CLT. Indeed, the red curve, which is the load-settlement calculated assuming a constant loading velocity of 0.005 mm/min at the pile head, agrees with the green curve, which is the load-settlement curve derived from the CLT when the velocity 0.005 mm/min is used as criterion to increase the load.

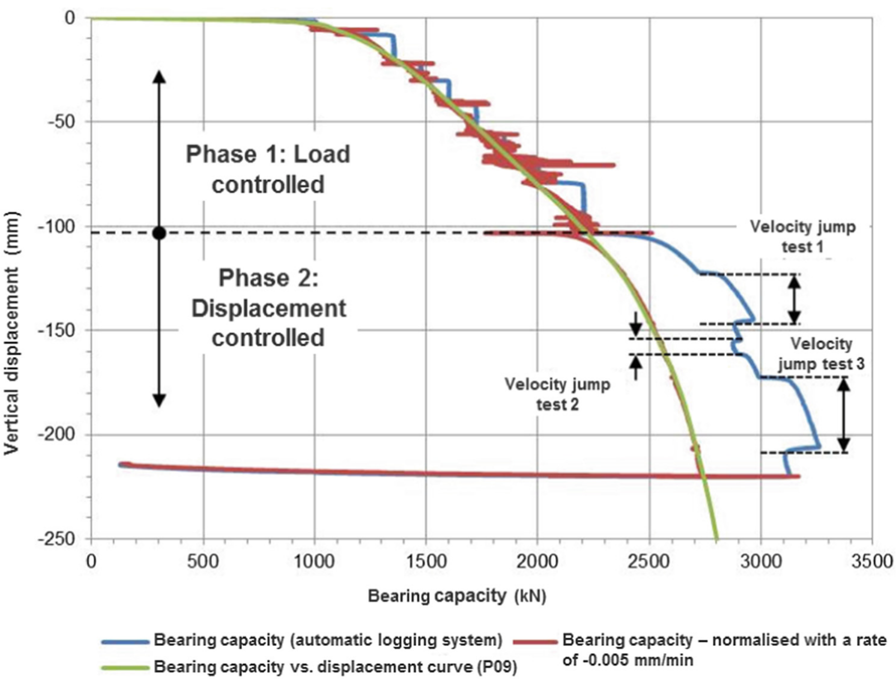

Fig. 10. Pile load vs. pile head settlement for the CLT and CRT phases for pile P09.

4.6 Results of the PLT

The comparison of the results of the three test piles in Fig. 11 shows, as expected, that the 60 m pile reached the highest bearing capacity of 6.5 MN at the displacement of approx. 0.1 D. The bearing capacities of the 30 m long piles were 3.2 MN (P09) and 2.2 MN (P10). This indicates that the pile capacity could be increased by approximately 30% by the proposed soil improvement. The CRT phase shows that even at pile displacement larger than 0.1 D, significant additional pile resistances can be still mobilised at expenses of an increase in the deformation velocity. Since the base resistance is similar for the three piles, the differences in the pile capacities originate in the skin friction, as seen in Fig. 12.

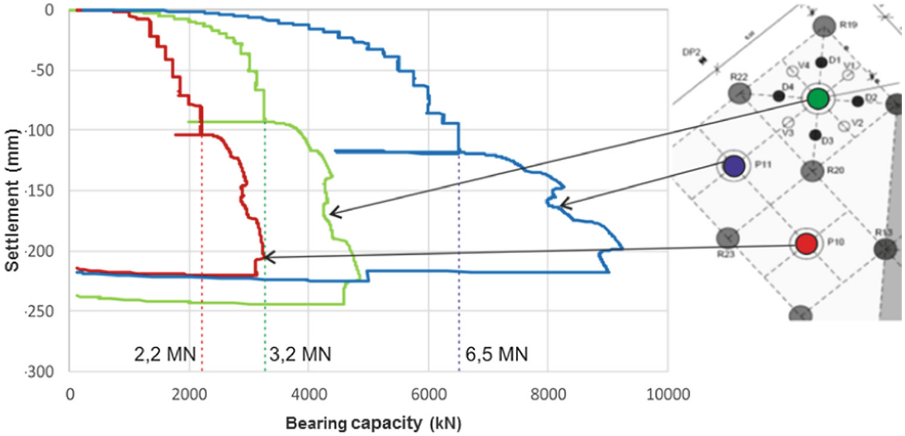

Fig. 11. Comparison of the bearing capacity-settlement lines of the test piles.

From the evaluation of the individual measurement cross-sections, the (depth-dependent) skin friction and the end bearing pressure were determined (Fig. 12). The skin friction reaches its maximum value at pile head displacements of 15 mm to 30 mm. The end bearing of all three piles increases almost linearly with the pile displacement to about 1,000 kN (P09 and P11) or 900 kN (P10) and does not appears to be fully mobilised at the end of the load-controlled phase. Despite a depth of almost double the piles P09 and P10, the mobilised tip resistance of pile P11 is still about 1,000 kN, compared to a similar value of 900 kN for P10 with a length of only 30 m. This result indicates that the end bearing is mainly controlled by the installation-related disturbance of the sensitive Seeton.

The "healing effect" of the soil improvement can be seen in the evaluation of the skin friction of the two 30 m piles with recorded values of about 25 kN/m^2 for P09, compared to 15 kN/m^2 for P10. Due to the soil improvement, the end bearing behaviour of P09 is lightly stiffer (with a displacement of 900 kN at 85 mm instead of 100 mm). The average skin friction is 25 kN/m^2 for P11 (60 m) and is thus higher than 15 kN/m^2 for P10. The fact that the mean skin friction of the 60 m pile is greater than the value of the 30 m pile is consistent with the increase of the shear strength with the depth indicated by the results of the field and laboratory tests.

Taking into account safety factors relating to the statistical scattering of the data from EA-Piles, characteristic values of the pile resistances could be reliably derived from the results of the third pile testing campaign.

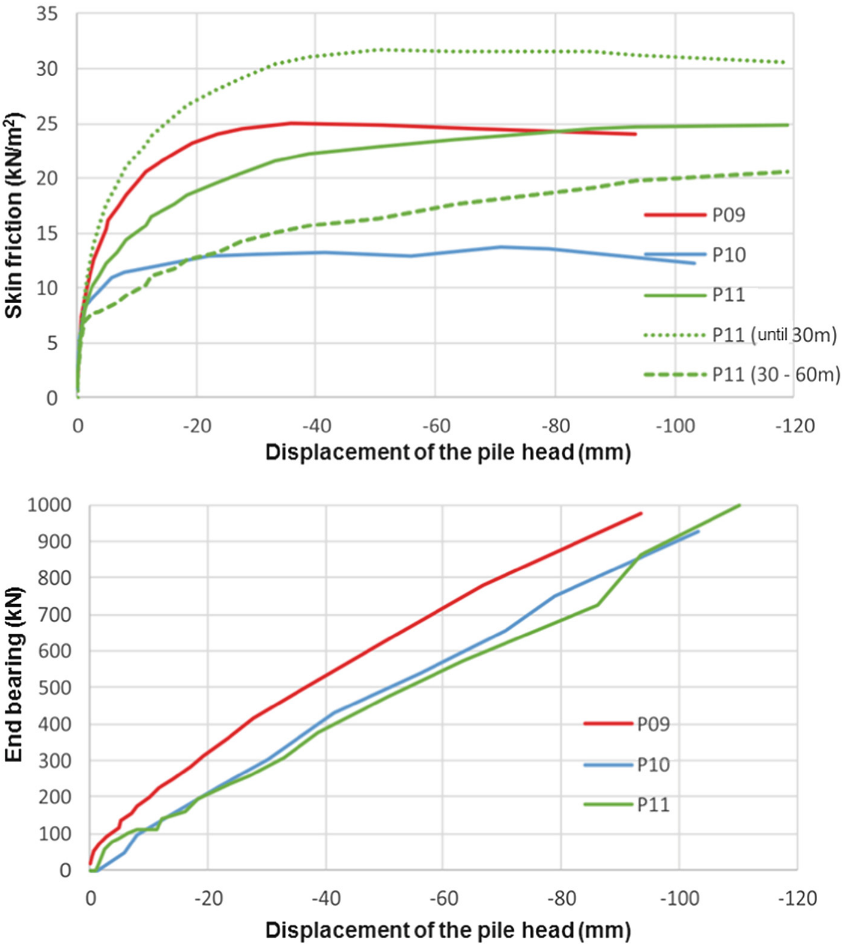

Fig. 12. Comparison of the mean skin friction (top) and the end bearing (bottom) over the head displacement of the three test piles in the CLT phase.

5 Foundation Design

On the basis of the test load results, two technically feasible alternatives for the foundation of the pylons (design vertical load $E_{v,d} \approx 80$ MN, characteristic vertical permanent load $G_k \approx 49$ MN, characteristic vertical traffic load $Q_k \approx 8$ MN) were identified. These options are limited due to the fact that the dimensions of the pile cap (15 m × 15 m) cannot be increased due to site constraints. The first foundation alternative is a classical pile foundation. In order to reduce the group effect of the piles and to avoid excessive disturbance of the subsoil during pile construction, 14 piles with a diameter of 1.2 m, a centre-to-centre distance of 4.5 m and a length of 65 m are specified. Under the characteristic load, a settlement of the single piles of about 8 mm can be estimated from the results of the pile tests. The settlement of the pile group for the permanent loads were estimated to be 3 cm to 4 cm using a simplified approach based on analytical solutions to the theory of elasticity with the program ELPLA 10.

The second alternative is a mixed foundation (Fig. 13), in which the loads are transferred through the piles, the pile cap and the soil improvement. In this foundation type, the bored piles are installed first, followed by the vertical drains and finally the unreinforced displacement piles, following the same sequence as for test pile P09. The displacement piles cause a consolidation of the subsoil and lead to an increase of the effective stress of the soil around the pile, which in turn increases the skin friction of the piles. The vertical drains enable a rapid dissipation of the excess pore water pressure generated by the soil displacement and thus a rapid consolidation of the Seeton. The length of the displacement piles is limited due to the method of installation and available equipment to approx. 50 m.

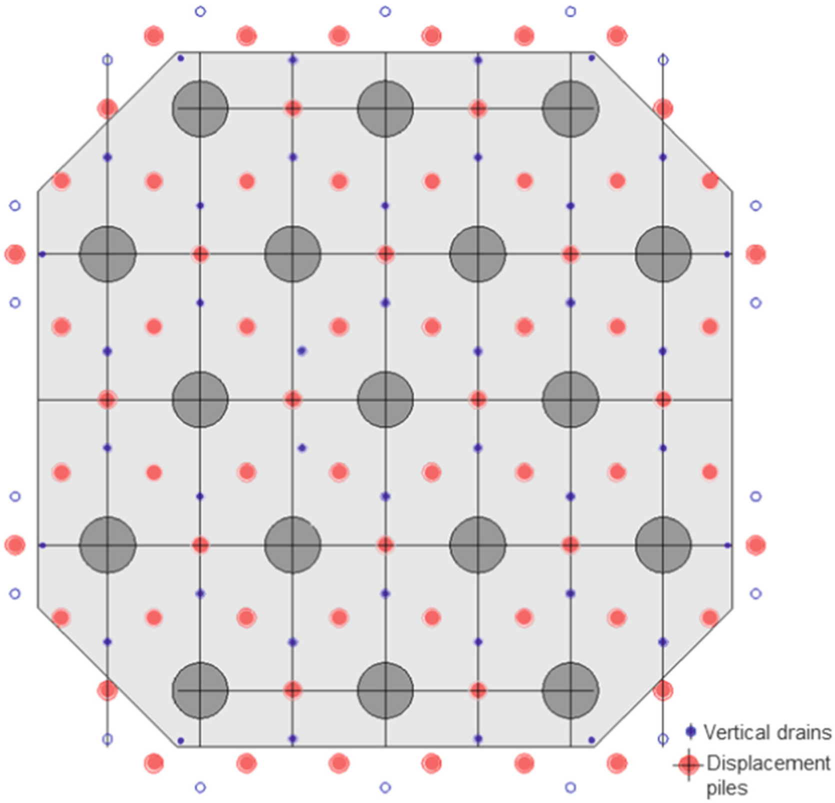

Fig. 13. Plan view of the foundation and layout of bored piles, displacement piles and vertical drains for the second alternative.

The single pile was designed in accordance with the DIN EN 1997-1:2014 and the DIN 1054:2010 for the portion of the load to be carried by the piles. Additionally, the ultimate limit state check of the bearing capacity of the pile group was performed for the total load, replacing the pile group by a single ‘replacement pile’ in accordance with

DIN EN 1997-1 and DIN 1054. The displacement piles are only intended to improve the subsoil and therefore no separate limit state verifications need to be performed.

From a geotechnical point of view, the mixed foundation was regarded as the more robust foundation type. The shorter piles reduce the risk of a disturbance to the subsoil during construction. In addition, the foundation behaviour is less dependent on the load bearing behaviour of the individual piles than the pure bored pile foundation variation. The displacement piles improve and homogenise the subsoil and counteract the installation-related disturbances.

6 Prediction of the Deformation Behaviour of the Mixed Foundation

The proportional characteristic load transferred through the pile cap and the piles as well as the deformation of the foundation is dependent on the soil-foundation interaction and can be calculated with the finite element (FE) method. The numerical modelling is thus the basis for the observation method and the planning of potential rehabilitation measures for the case of inadmissible settlements. ABAQUS v2017 was used for the FE simulations and the Seeton was modelled with a visco-hypoplastic model proposed by Niemunis (2003).

6.1 Material Model Parameter Calibration and Validation

The model parameters were either determined on the basis of the results of the laboratory tests or estimated based on index tests on remoulded samples. The ability of the constitutive model to predict the in-situ behaviour of the lacustrine clay or "Seeton" parameter was checked by comparing numerical predictions of the cone penetration and pressiometer test results with the values measured in the field. The visco-hypoplastic parameters for the lacustrine clay used in the numerical simulations are:

Parameters	Description	Value
e_r	Reference void ratio for p_r = 100 kN/m^2 at the reference rate	0.86
λ	Compression index (virgin compression)	0.04
κ	Swelling index (unloading-reloading)	0.01
β_R	Shape of the yield surface	0.5
I_v	Viscosity index	0.03
D_r	Reference creep rate	1e−7 m/s
φ'_c	Friction angle	30°
m_2	Intergranular strain parameters	5.0
m_5		5.0
R_{max}		1E−4
β_x		0.2
χ		1.5

The numerical and experimental results of oedometric compression tests and undrained triaxial compression tests are compared in Figs. 14 and 15. In Fig. 16, the relationship between the radial pressure and the normalised radial displacement r/r_0 (r_0, r: initial and current radius of the cavity), as derived from the pressiometer tests, are compared with the numerical solution of the cylindrical cavity expansion problem under undrained conditions for depths of 10 m–20 m and 30 m–40 m. In the cavity expansion model, the mechanical behaviour of the Seeton is simulated by the visco-hypoplastic model with the model parameter given above. The initial state of stress of the soil is defined by the vertical stress σ_z resulting from the overburden, the radial and annular stresses:

$$\sigma_{\theta,r}/\sigma_z = K_0 = 1 - \sin\varphi'.$$

In addition, an overconsolidation ratio OCR = 1.5 was assumed for the in-situ state, which has been determined with the constitutive model for an estimated age of the Seeton of 10.000 years. Furthermore, the expected creep settlements of the Seeton for free-field conditions in the next 100 years starting with OCR = 1.5 was analysed. The calculated settlement of a few centimetres during this period of time was considered realistic, as large subsidences of the ground surface have not been observed in the region of Rosenheim so far. In Fig. 16 only the numerical results for the upper and

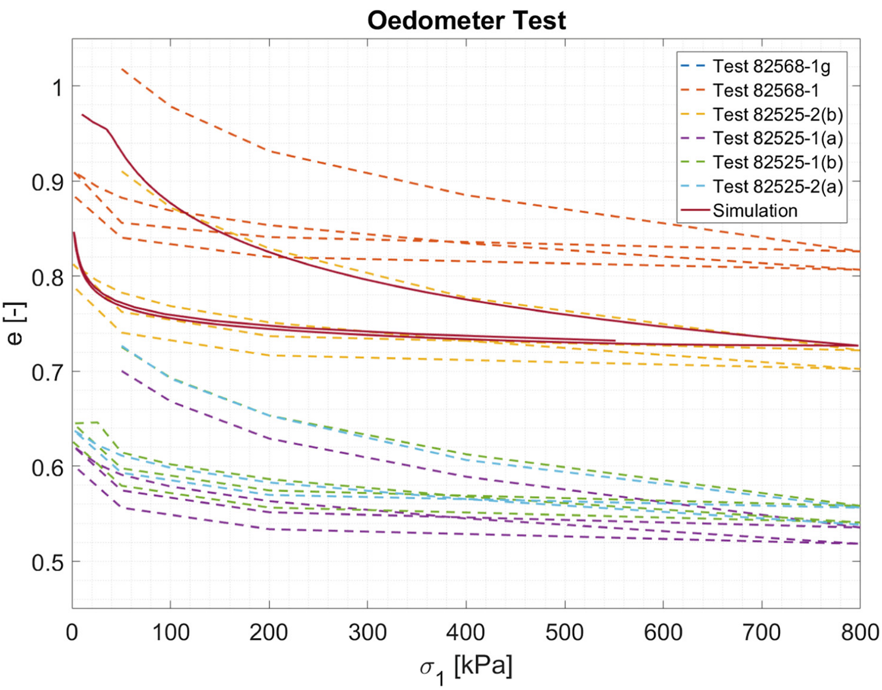

Fig. 14. Oedometric compression: void ratio versus effective vertical stress from laboratory tests and numerical element test simulations with the visco-hypoplastic constitutive model.

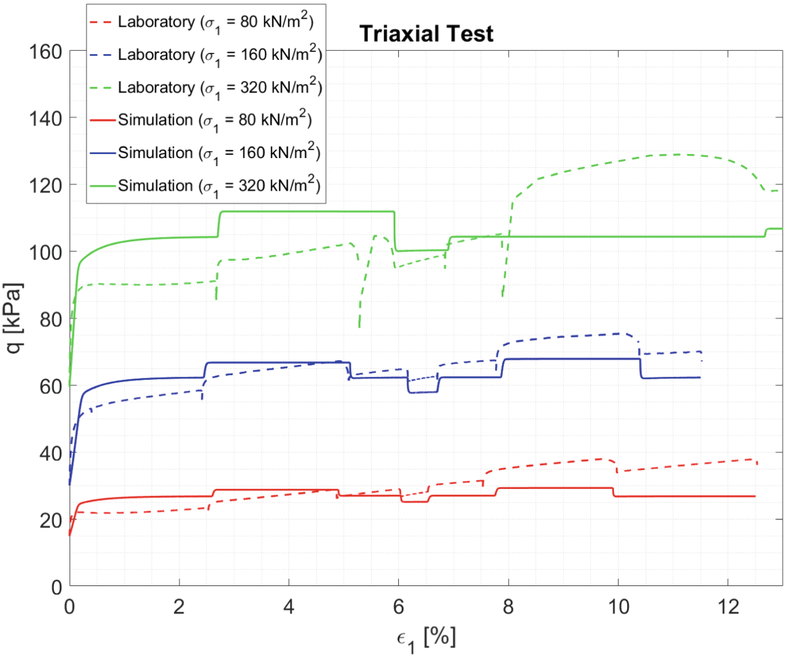

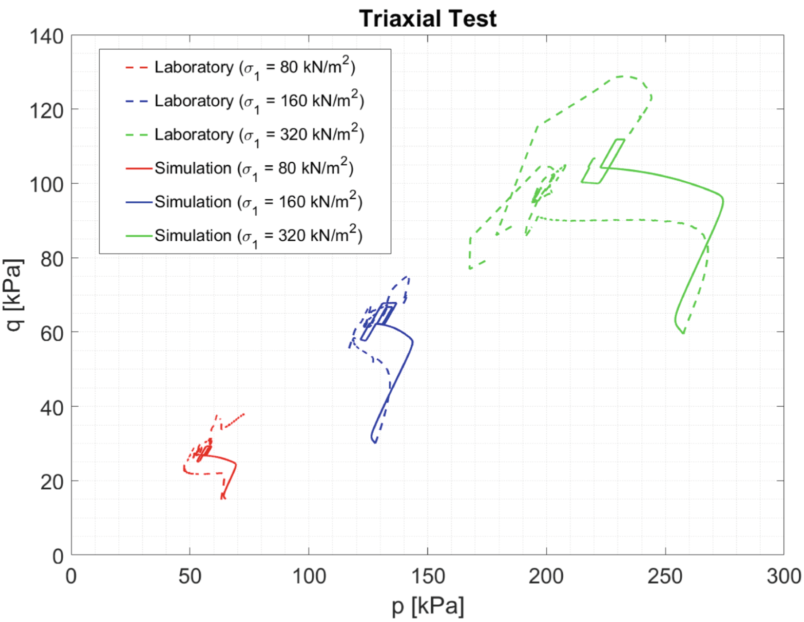

Fig. 15. Undrained triaxial compression: deviatoric stresses versus axial strain (top), deviatoric stresses versus mean stress (bottom) from laboratory tests and numerical element test simulations with the visco-hypoplastic constitutive model.

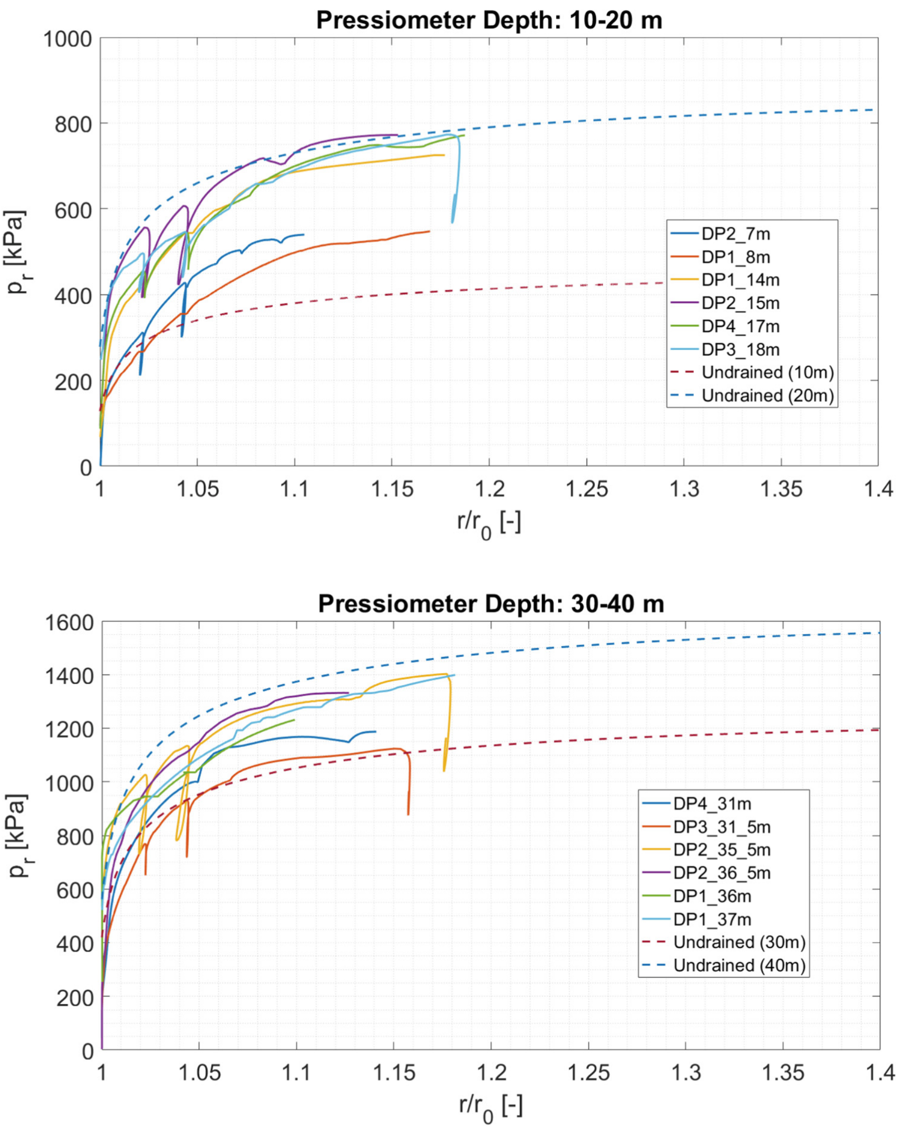

Fig. 16. Comparison of experimental pressure-expansion curves obtained with the cone-pressiometer testing device (CPTM) with the prediction using a cylindrical cavity expansion model for the depth intervals 10–20 m (top) and 30–40 m (bottom).

lower values of the considered depth range have been plotted. As it can be seen, both the laboratory and pressiometer tests can be realistically simulated by the constitutive model.

6.2 Simulation of a Single Pile Load Test (P09)

The prediction of the load-settlement response of the mixed foundation is based on the back-calculation of the single pile loading tests - in particular the results of pile P09. The disturbance of the subsoil and the installation-related reduction of the skin friction was taken into account by modelling the excavation of the borehole and the concrete pouring process. Thereby, a radial displacement of the borehole wall towards the vertical axis was prescribed, in order to induce a stress relaxation in the vicinity of the pile. By varying the magnitude and the distribution of the applied displacements, the relaxation (disturbance) required to reproduce satisfactorily both the creep deformation in the CLT phase and the rate-dependent load-settlement behaviour in the CRT phase was determined with the FE-model of the single pile shown in Fig. 17.

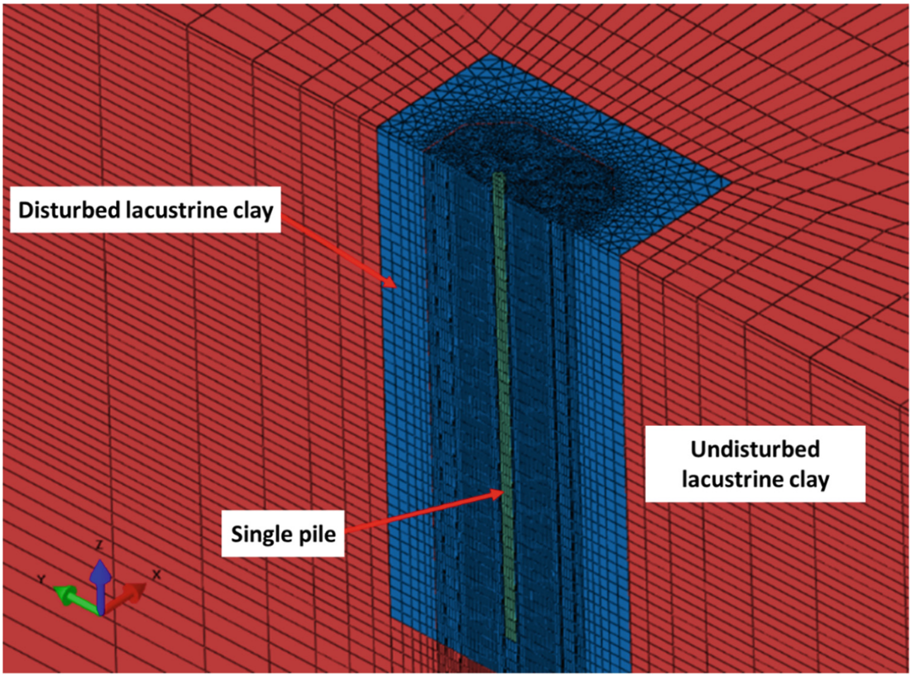

Fig. 17. 3D FE-Model of the single pile with soil improvement (P09) with the same mesh discretisation as the pile group model.

The result of the simulation of the time-dependent behaviour of the pile P09 during the two test phases along with the results of the PLT using the 3D FE-model of the single pile are shown in Fig. 18. A comparison of the numerical and experimental determined pile head displacements for four constant load stages is depicted in Fig. 19. As it can be seen in both figures, the proposed technique to account for pile installation in the numerical simulation enables the back-analysis of the time-dependent behaviour of the single pile realistically, although no relative displacement between the soil and the pile can occur in the numerical model.

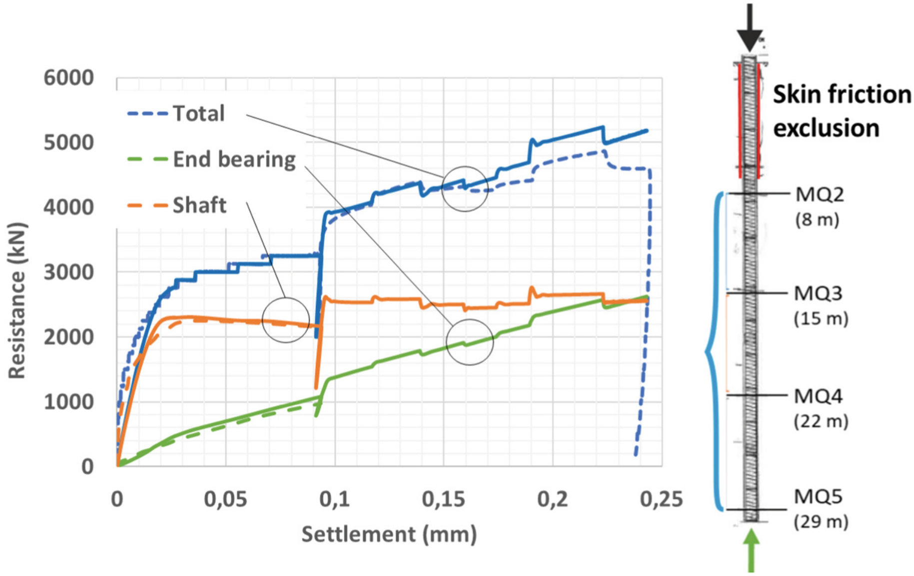

Fig. 18. Comparison of the results of the pile test for P09 (dashed lines) with the results of the FE modelling (continuous lines): pile load (black), the shaft resistance (blue) and end bearing resistance (green) as a function of the settlements at the pile head.

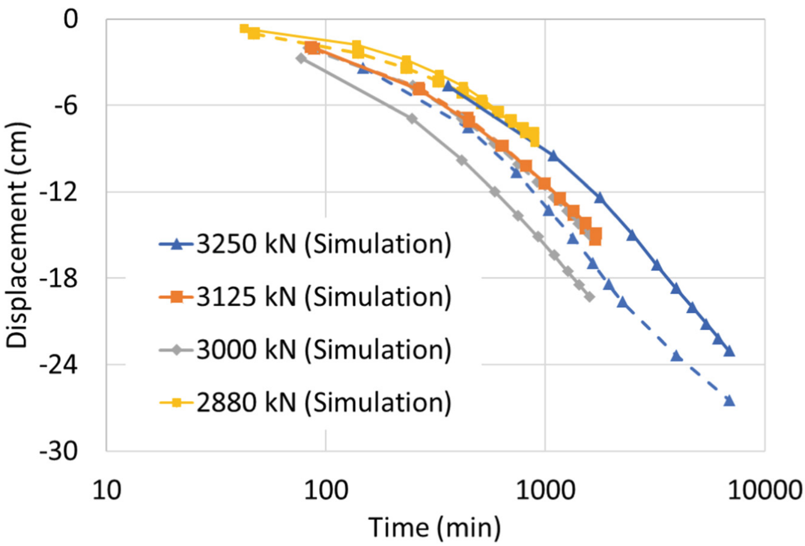

Fig. 19. Settlement of the pile head versus the relative time for the last four load increments: Comparison of results of the pile loading test (dashed lines) and the numerical simulations for P09 (continuous lines).

6.3 Simulation of the Pylon Foundation

Based on the simulation of the single pile loading test, and using the same 3D mesh, the behaviour of the pile group corresponding to the pylon foundation of the cable stayed bridge was simulated using the same method of relaxation of the soil surrounding the pile, in order to capture the effect of the soil disturbance.

Figure 20 shows the FE model for the pylon with the pile group and the improved subsoil (left), as well as the contour of the calculated deformations at the end of construction (right). The disturbance due to pile installation was considered in the same way as in the numerical analysis of the single pile. The soil improvement induced by the displacement piles was taken into account by increasing the stiffness of the soil between the piles. In order to estimate this stiffness the load-settlement behaviour of an axisymmetric model consisting of a column in the axis and soil around it was calculated considering displacement conditions corresponding to a rigid foundation. Then, the soil stiffness with a comparable load-settlement behaviour was calibrated based on the same axisymmetric model with the same dimensions and boundary conditions but without the column.

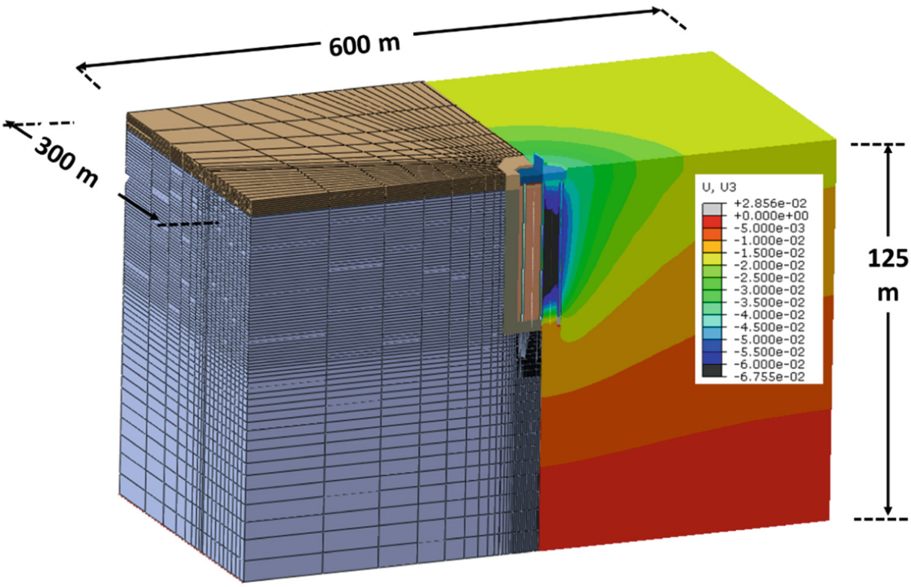

Fig. 20. FE model Pylon view of the mesh (left) and the resulting displacement after 40 years in operation (right).

The FE model of the pylon predicts a maximum foundation settlement of about 6–7 cm after 40 years of operation. The large concentration of the soil deformation in the area of the pile group and the significantly lower settlements of the surrounding area is clearly visible. The development of the foundation settlement predicted by the model for an operation time of 40 years is presented in Fig. 21. A monitoring program will be implemented to track the soil and the foundation deformations during construction.

Based on the data from the monitoring, the FE-model and the prediction will be validated and if required, adjusted and improved.

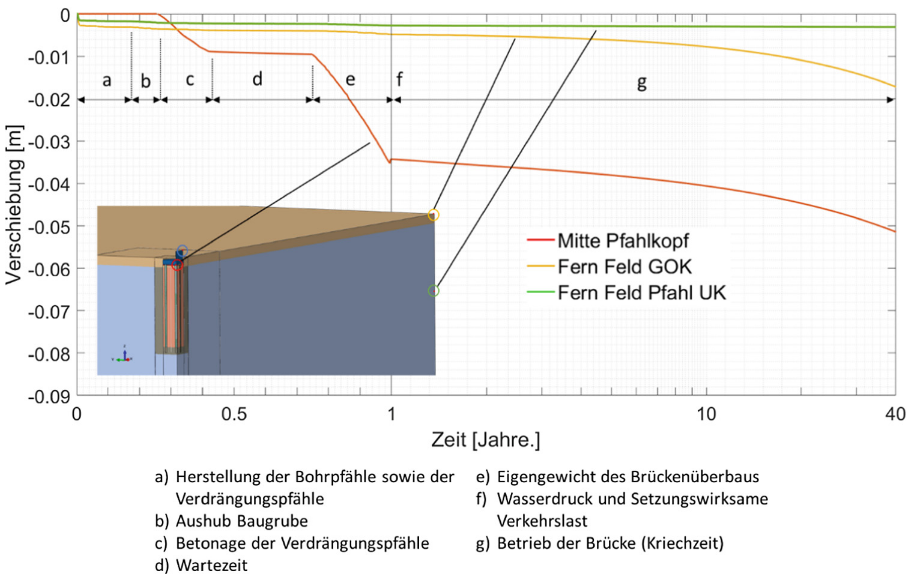

Fig. 21. Evolution of the vertical displacements of the centre of the pylon foundation. For easier visualization, the time axis is linear until in the end of construction (1 year) and logarithmic thereafter (from 1 to 40 years).

7 Final Remarks

Geotechnical solutions in sensitive fine-grained soils, such as the Rosenheim Seeton, require special demands on the investigation of the subsoil, the planning and the construction. The comprehensive subsoil investigations, including laboratory and field tests, enabled the geotechnical characterisation and parameter calibration necessary for modelling the time-dependent mechanical behaviour of the Seeton. The results of the 3rd pile testing campaign illustrate the pronounced sensitivity of the fine-grained soil and highlight the special precautions that must be taken during pile construction to reliably, and reproducibly achieve the pile resistance required to transfer the bridge loads to the subsoils.

A mixed pile-raft foundation was proposed as an alternative to a classical piled foundation, which was considered infeasible from a technical and economical point of view. In order to counteract the effect of soil disturbances due to pile construction and to improve the stiffness of the soil between the bored piles, vertical drains and displacements piles in this sequence, will be installed after the piles.

The time-dependent load-settlement behaviour of a single pile, also including the displacement piles and the vertical drains was investigated by means of high quality pile loading tests. Based on the back-calculation of the single pile tests, a 3D FE Model of the mixed foundation, which considers the time-dependent behaviour of the Seeton and the load settlement behaviour of the single pile, was developed and used to predict time-dependent behaviour of the foundation.

In order to mitigate the geotechnical risks associated with the Seeton and according to the current design, the superstructure can be lifted by means of hydraulic jacks, if inadmissible settlements and differential settlements occur during operation. The lifting system will allow an individual compensation of the settlement of the pylons and piers several centimetres.

In order to control the performance of the foundations, a geotechnical monitoring system will be implemented during construction and operation of the bridges. In accordance with the observation method, the results of the monitoring will be used to validate the numerical model of the foundation and to improve the prediction of foundation settlements. The numerical predictions of the time-dependent foundation settlements combined with the monitoring data will be the basis for decision making regarding the lifting of the superstructure.

References

EA-Piles, Empfehlungen des Arbeitskreises “Pfähle”. Deutsche Gesellschaft für Geotechnik, 2nd edn. Ernst & Sohn Publisher (2012)

Niemunis, A.: Extended hypoplastic models for soils, Heft 34. Veröffentlichungen des IGB der Ruhr-Universität Bochum (2003)

Krieg, S.: Viskoses Bodenverhalten von Mudden, Seeton und Klei, Heft 150. Veröffentlichungen des IBF, Karlsruhe Institute of Technologie (2000)

Krieg, S., Goldscheider, M.: Bodenviskosität und ihr Einfluss auf das Tragverhalten von Pfählen. Bautechnik 75, vol. 10, pp. 806–820 (1998)

Leinenkugel, H.J.: Deformations- und Festigkeitsverhalten bindiger Erdstoffe. Experimentelle Ergebnisse und ihre physikalische Deutung, Heft 66. Veröffentlichungen des IBF, Karlsruhe Institute of Technologie (1976)

Hansbo, S.: A new approach to the determination of the shear strength of clay by the fall-cone test. In: Proceedings of the Royal Swedish Geotechnical Institute, vol. 14 (1957)